Vision Res. Vol. 33, No. 1, pp. 105–116, 1993
Printed in Great Britain.

0042-6989/93 $5.00 + 0.00

Spatial Reconstruction of Signals from Short-Wavelength Cones

DAVID H. BRAINARD,*† DAVID R. WILLIAMS*

Received 18 September 1991; in revised form 11 May 1992

Because the retinal cone mosaic samples an image only at discrete locations, our continuous visual percept must arise from a spatial reconstruction process. How this process combines information from the three cone types is presently unclear. To investigate, we asked whether L and M cone information can modify the visual system's reconstruction of signals from S cones. In Expt 1, we used a matching paradigm to measure the effect of L and M cone information on filling-in at the foveal tritanopic area. We found that a small luminance disk superimposed at the tritanopic area decreases the amount of filling-in, showing that the reconstruction of S cone signals can be influenced by the spatial pattern seen by the L and M cones. In Expt 2, we asked whether L and M cone information can modify the splotchy low-frequency alias seen when an observer views fine S cone gratings. Here there was no evidence for an interaction. We conclude that though L and M cone information can influence the visual system's reconstruction of S cone signals, this influence may be confined to relatively coarse spatial patterns.

Reconstruction Filling-in Aliasing Short-wavelength cones Interpolation

INTRODUCTION

General considerations

A fundamental task confronting the visual system is to estimate the properties of objects in the world. This task is difficult because the visual system has incomplete information about these object properties. The information may be incomplete because the retinal image itself is improverished, as when one object is partially occluded by another. Nonetheless, the visual system is capable of estimating properties of the occluded parts (Kanisza, 1979; Nyman & Laurinen, 1982; Marr, 1982; Kersten, 1987; Cavanagh, 1987; Koh & Maloney, 1988; Nakayama, Shimojo & Silverman, 1989).

Alternatively, the information may be available in the retinal image but subsequently lost. For example, the portion of the image that falls on the optic disk is not available for further processing. In this case, our visual system hides this loss from subjective experience by filling a percept into the blind area (e.g. Helmholtz, 1896; Walls, 1954; Kawabata, 1983). Similar filling-in effects are observed for the rod-free area under scotopic conditions (Walls, 1954) and for the central fovea under conditions that isolate the S cones (Williams, MacLeod & Hayhoe, 1981a).

The information loss at these retinal blind areas is caused by spatial sampling. Images that differ only in retinal locations where there are no photoreceptors are indistinguishable to the visual system, since they produce identical responses in all of the available photoreceptors. Such images are *aliases* of one another, and we say that *aliasing* occurs when a stimulus is perceived as one of its aliases. The various filling-in phenomena noted above all demonstrate spatial aliasing.

Spatial aliasing occurs because the photoreceptors sample the retinal image at discrete spatial locations. In the above examples, the sampling is rather coarse. At a much finer spatial scale, the gaps between individual photoreceptors can produce aliasing. Physically distinct images can generate identical receptor responses if they vary only in the blind areas between individual photoreceptors.‡ The effect of these small blind areas has been demonstrated empirically for the foveal and extrafoveal cone mosaic. When high spatial-frequency gratings are imaged on the retina, observers experience a low spatial-frequency percept which corresponds to an alias of the grating stimulus (Williams, 1985, 1988; Coletta & Williams, 1987; Coletta, Williams & Tiana, 1990). Figure 1 illustrates pairs of aliases for one-dimensional stimuli.

The set of aliases of any particular stimulus is determined by how the image is sampled. Since the members of this set are identical at the sample points, they must all be perceived identically. How they are perceived is

*Center for Visual Science, 274 Meliora Hall, University of Rochester, Rochester, NY 14627, U.S.A.
†Present address: Department of Psychology, University of California, Santa Barbara, CA 93106, U.S.A.

‡Strictly speaking, this statement applies to a mosaic containing punctate receptors with infinitesimal entrance apertures. We can, however, accurately treat the sampling by real receptors in two steps (Pratt, 1978). First we convolve the retinal image with the receptor aperture. We then sample the results with punctate receptors. Two images will be indistinguishable when the output of the convolution varies only in the gaps between the punctate receptors.

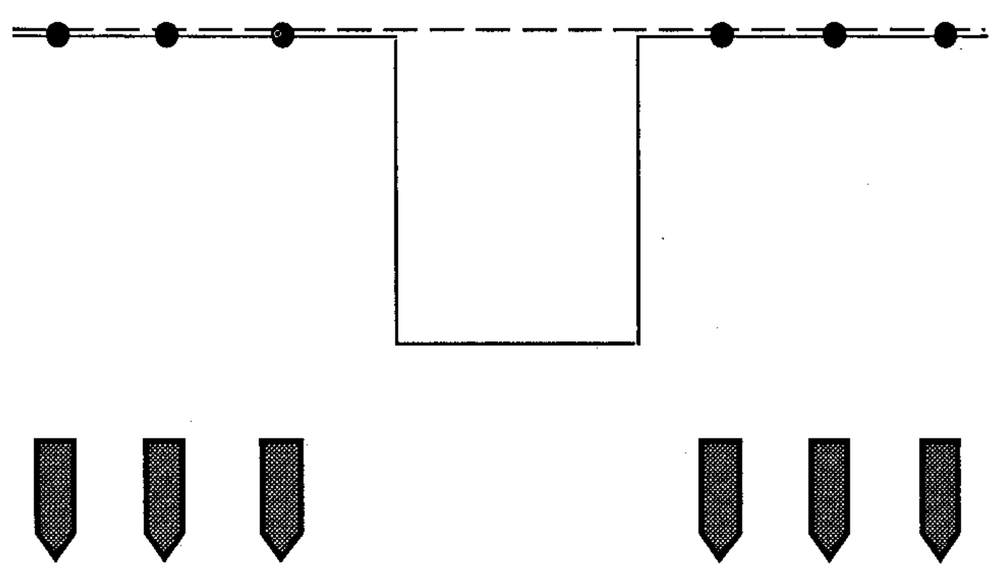

FIGURE 1. Two one-dimensional examples of alias pairs. The shaded polygons represent the locations of cones in a one-dimensional retina. Above each set of cones we plot the intensity profile of two one-dimensional images. The intensity at cone locations is indicated by a solid dot. The top panel shows how aliasing can occur at an extended blind area, such as the optic disk or foveal tritanopic area. The two image profiles, shown by the solid and dashed lines, are identical outside the blind area, but differ within it. The bottom panel shows aliasing at a fine spatial scale. As before, the two patterns are identical at all cone locations but differ at locations between the cones.

determined by subsequent visual processing. We use the term *reconstruction* to refer to the processes that estimate the missing information. Reconstruction can be thought of as the rule by which the visual system chooses one privileged stimulus from each set of aliases. The percept that fills into a blind retinal area reflects the operation of a reconstruction process, as does the low frequency percept associated with undersampled fine gratings.

Sampling of S cones

The trichromacy of human vision is mediated by three classes of cones, differentiated by their spectral responsivities. The individual cones are arranged as three interleaved submosaics, each consisting of L, M, or S cones. Because the visual system contains only three classes of cones, we can specify the stimulus by describing the spatial and temporal modulations seen by each of the cone classes (see e.g. Wyszecki & Stiles, 1982). We call these the L, M, and S cone components of the stimulus.

There are two important features of the S cone submosaic. First, there are no S cones at the very center of the fovea, a region which we refer to as the tritanopic area. Both psychophysical and anatomical studies indicate that this area has a diameter of approx. 20′ of visual angle (Williams *et al.*, 1981a, b; deMonasterio, McCrane, Newlander & Schein, 1985; Curcio, Allen, Sloan, Lerea, Jurley, Klock & Milam, 1991). These studies also indicate that the S cone submosaic is by far the sparsest of the three submosaics, accounting for only about 7% of the total number of cones. These two features of the S cone submosaic allow us to reveal the action of reconstruction processes more easily for S cone isolated stimuli than for stimuli that stimulate all three classes of cones.

In most previous studies of spatial aliasing by the S cones (Williams *et al.*, 1981a; Williams & Collier, 1983; Williams, Collier & Thompson, 1983; Williams, Sekiguchi, Haake, Brainard & Packer, 1991), the stimulus was arranged so that there was little or no modulation of the L and M cones. The results of these studies therefore reflect how the system uses the available S cone responses to reconstruct the S cone stimulus component. One possibility is that, in general, this reconstruction depends only on the S cone responses. We call this possibility separate S cone reconstruction. This is not the only possibility. A reconstruction procedure could use the responses of all three cone classes to estimate the S cone stimulus component. Under many circumstances, the three stimulus components are highly correlated. For example, any time the stimulus is an intensity modulation, the response of each stimulus component reliably predicts the other two. This observation suggests that the visual system might improve the accuracy of its S cone reconstructions through the use of L and M cone signals. This idea is consistent with the commonly accepted notion that luminance boundaries can constrain the spread of chromatic percepts (e.g. Gregory, 1977; Boynton, Hayhoe & MacLeod, 1977; Eskew, 1989; Cole, Stromeyer & Kronauer, 1990).

In this paper, we investigate whether the visual system's S cone reconstruction depends on signals originating in the L and M cones. In Expt 1, we develop a matching paradigm to quantify the amount of tritanopic area filling-in. We then measure how L and M cone signals affect this filling-in. In Expt 2, we ask whether L and M cone signals can alter the splotchy low frequency percept associated with fine S cone gratings.

EXPERIMENT 1—TRITANOPIC AREA

Overview

Williams *et al.* (1981a) showed that an annulus seen only by the S cones will fill-in and appear uniform if its inner diameter lies within the foveal tritanopic area. The purpose of Expt 1 was to measure whether this filling-in is affected by L and M cone information. The stimulus was formed as the superposition of a long-wavelength background, a short-wavelength component, and a luminance component, as shown in Fig. 2. The long-

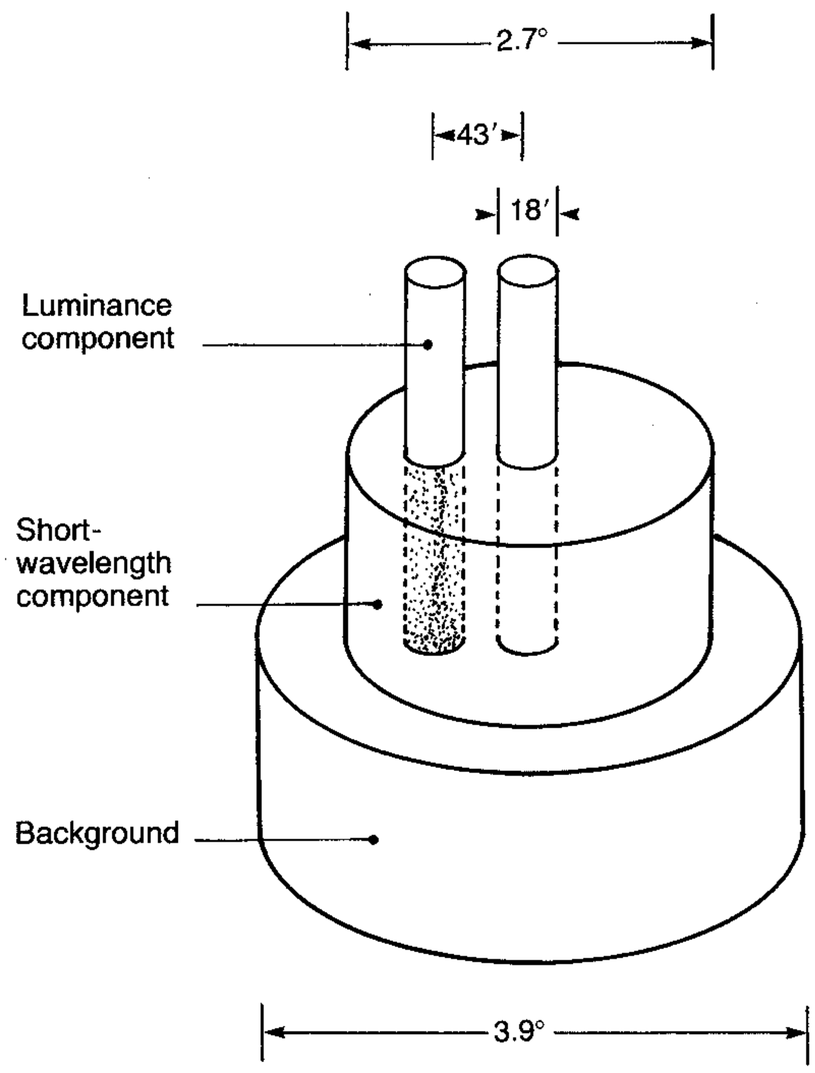

FIGURE 2. Schematic of Expt 1 stimulus. The stimulus was formed as the superposition of a long-wavelength background, a short-wavelength component, and a luminance component. The background consisted of a spatially uniform long-wavelength field subtending 3.9 deg of visual angle. Its CIE 1931 chromaticity coordinates were $x = 0.53$, $y = 0.47$. The background luminance was approx. 1400 cd/m^2 (9896.0 td). The short-wavelength component was made up of 440 nm monochromatic light. It consisted of a spatially uniform 2.7 deg circular field containing two small 18 min diameter disks. One disk was located at the center of the short-wavelength field. The second disk was located 43 min eccentric on the nasal side of the short-wavelength field. During the experiment, the intensity of one of these disks was set to zero, while the intensity of the other was under the observer's control. In the figure, one of the disks is shaded to indicate that its intensity could be adjusted. (In some experimental conditions, the roles of the two disks were reversed.) The luminance of the uniform part of the short-wavelength field was approx. 0.2 cd/m^2 (1.4 td). The luminance component consisted of two identical 18 min circular disks, superimposed in register with the disks of the short-wavelength component. The chromaticity of these disks matched the background, while their luminance was under experimental control. Exact calibration values varied from session to session and are reported with the results. Not shown is a fixation cross-hair positioned near the edge of the background field. The figure is not drawn to scale.

wavelength background allowed the short-wavelength component to be seen only with the S cones. The short-wavelength component was a spatially uniform circular field containing two circular regions, 18 min in diameter, whose intensity could be controlled independently. During the experiment, the observer fixated one of these disks, which we call the *foveal disk*. The intensity of this disk was set to zero. The intensity of the other disk was under the observer's control. We call this the *comparison disk*. The observer's task was to adjust the intensity of the comparison disk until it matched the foveal disk in color appearance. Observers set these appearance matches with and without a *luminance component*. The luminance component consisted of two identical 18 min circular disks, superimposed in register with the disks of the short-wavelength component. The spectral composition of the luminance component was the same as the long-wavelength background. Matches set with no luminance component measured the amount of tritanopic area filling-in when the S cones operated in isolation. Matches set with the luminance component measured the influence of L and M cone information on S cone filling-in.

Apparatus and stimulus details

The stimuli were presented using the apparatus shown in Fig. 3.

Background. The background was formed by light reflected from a front projection screen. Three slide projectors were used to project light onto the screen. The reflected light passed through fieldstop FS1 and was relayed to the eye using mirror M1, beam-splitter BS1, and long-wavelength reflective dichroic mirror D1. Yellow-transmissive dichroic filter F1 and reflection from D1 removed short-wavelength light from the background. Fieldstop FS1 consisted of a 3.9 deg circular aperture and a piece of plate glass which contained a fixation cross-hair. The cross-hair was positioned near the edge of the aperture and served to help the observer maintain accommodation. It did not obstruct the foveal and comparison disks. A small dim speck of dust located on the glass plate served as a fixation target. Heat absorbing glass was used to protect the eye from i.r. radiation.

Short-wavelength component. The short-wavelength component was generated by the blue phosphor of a

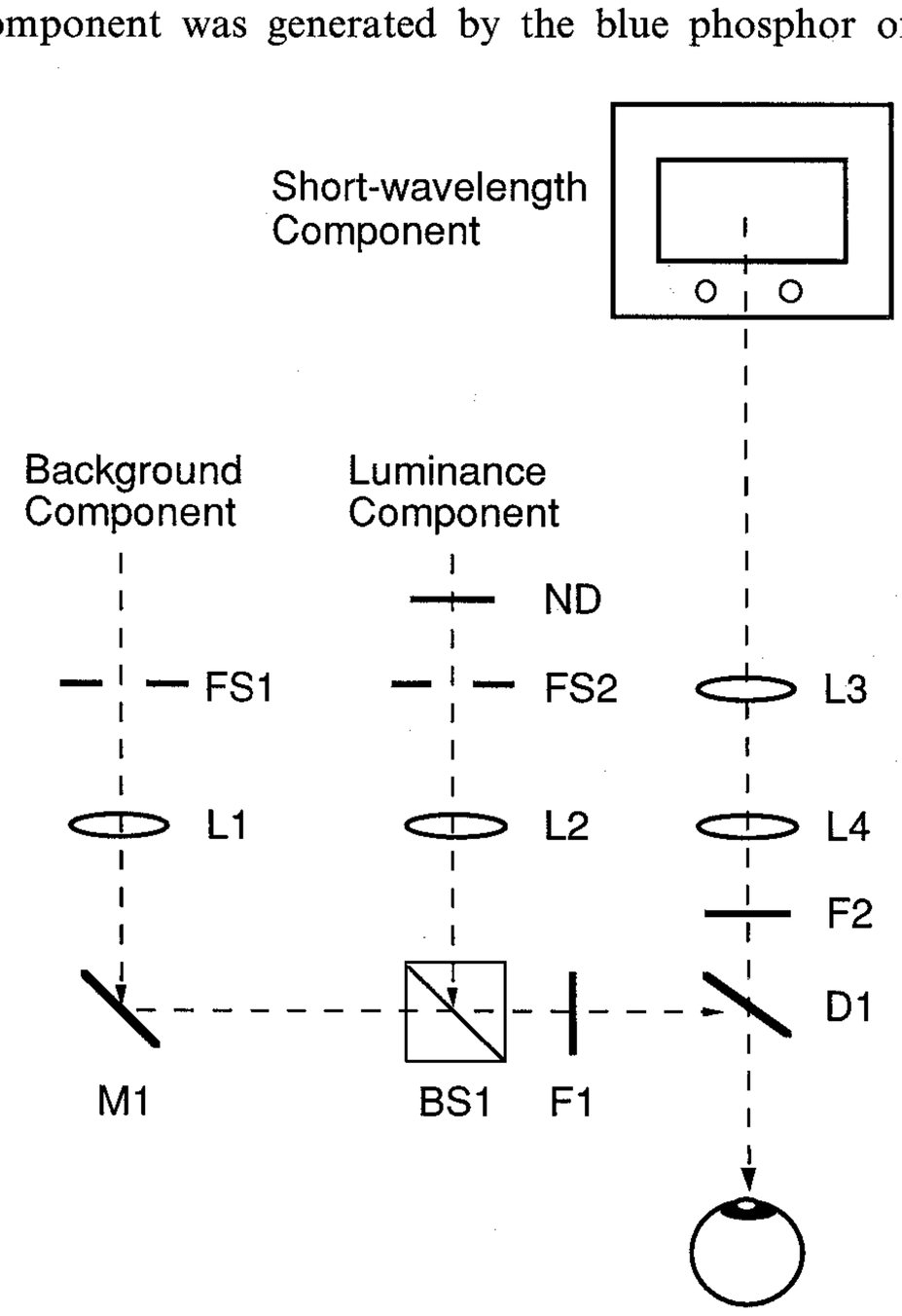

FIGURE 3. Experiment 1 apparatus. See description in the text. For clarity, one relay mirror has been omitted from the diagram, and the apparatus is shown with a more regular geometry than was actually used. Also not shown are shutters that controlled the presentation of the short-wavelength and luminance components, a 3 mm artificial pupil placed in front of the observer's eye, and trial lenses.

Panasonic model CT 2081Y color monitor, controlled by a Pixar II image computer. The RGB control signals generated by the Pixar were converted to S-video monitor input signals by a Truevision VIDI/O converter box. The computer/monitor combination provided a 30 Hz interlaced display with a total spatial resolution of 484 rows by 640 columns.

Lens L3 ($f = 165$ mm) formed a real image of the monitor whose focal distance could be adjusted by varying the distance between the lens and the viewer. Lens L4 ($f = 500$ mm) relayed the image to the viewer. Lens L4 was placed one focal length from the eye. By adjusting the position of lens L3, the observer could focus the monitor image without large changes in magnification. Light from the monitor passed through 440 nm interference filter F2 and short-wavelength transmissive dichroic mirror D1.

Luminance component. The luminance component could be superimposed on the short-wavelength component using a second long-wavelength channel. The luminance component was combined with the background using beam-splitter BS1 and then relayed to the eye as shown. The spatial structure of the luminance component was controlled by the use of high-contrast slides (Kodak Ektagraphic HC film) placed at FS2. Filter F1 and reflection from dichroic mirror D1, common with the background channel, removed short-wavelength light from the luminance component. Neutral density filters or an occluder placed at ND controlled the intensity of the luminance component.

Calibration. The stimuli were calibrated using a Minolta Chromameter (model CS-100 with data processor model DP-101) interfaced to the Sun 3/50 host computer over a serial line. The chromameter provided measurements of the CIE 1931 *XYZ* tristimulus coordinates of any stimulus. Calibration measurements were used to correct the non-linear relation between video frame-buffer input values and resulting phosphor intensities.

S cone isolation. We constructed our stimulus so that the short-wavelength component would be visible only to the S cones. Our calibration measurements indicated that the central disk of short-wavelength component had a small luminance contrast: 0.023% with respect to Judd's (1951) modified luminance efficiency function (Wyszecki & Stiles, 1982). As the logic of our experiment does not require perfect S cone isolation, we did not perform direct tests to verify that our short-wavelength component was seen only by the S cones. For our purposes, it was sufficient to verify (see Results section) that our observers reported good filling-in of the central disk when there was no added luminance component.

Procedure

The observer clenched a dental impression and used an x–y–z stage to align his eye with respect to a 3 mm artificial pupil placed directly in front of the cornea. Trial lenses were used to correct refractive errors. To correct for the axial chromatic aberration of the eye, the observer adjusted the position of lens L3, field stop FS1, and field stop FS2 so that all three stimulus components were in sharp focus. One of the disks was chosen as the foveal disk, and observer aligned a suitable fixation point in the background (usually a small speck of dust) with this disk.

The background was presented steadily. The short-wavelength and luminance components were flashed together for 500 msec using mechanical shutters. The observer could present a flash whenever he or she wished by pressing a button. The observer's task was to adjust the intensity of the 440 nm light emitted at the comparison disk so that the appearance of the foveal and comparison disks matched. Four matches were generally set for each condition. For half of the matches the initial intensity of the comparison disk was set to a low density. For the other half the initial intensity was set to a high intensity. For each condition, we report the mean of the individual matches.

The authors (DHB and DRW) and a third experienced observer (MMH) participated in Expt 1.

Results

When there was no luminance component present, all three observers reported that the foveal disk appeared to fill-in completely on most trials. The central disk was easily visible when the observer fixated elsewhere during the stimulus presentation, which rules out the possibility that the disk was of insufficient size or contrast for the S cones to resolve. On a few trials, a small yellowish smudge was seen at the fovea, which we attribute to a failure to maintain precise fixation.* When the luminance component was above threshold, all three observers found it possible to judge whether the comparison disk appeared too bluish or too yellowish relative to the foveal disk. The resulting matches were quite reliable, although all observers reported some subjective variability in the relative appearance of the two regions from trial-to-trial. This variability may be due to variations in fixation. Observers were generally satisfied with the quality of the ultimate perceptual match.

Figure 4 shows the results of Expt 1. Each panel of the figure shows the results for one observer. The horizontal axis shows the contrast of the luminance component on a log scale. We defined contrast magnitude to be the difference of the maximum and minimum stimulus luminances, divided by their sum. A contrast of zero indicates that there was no luminance component present. A positive contrast denotes a luminance increment. The vertical axis shows the S cone contrast of the mean comparison disk match on a linear scale. We took the S cone contrast to be the contrast of short-wavelength comparison disk with respect to the short-wavelength

*Another possible cause of this smudge is that our stimulus conditions did not completely isolate the S cones. We think this is unlikely because our calibration measurements indicate that short-wavelength component produced negligible luminance contrast. In addition, the presence of a luminance artifact cannot easily explain the fact that the yellowish smudge was seen on only a small fraction of trials.

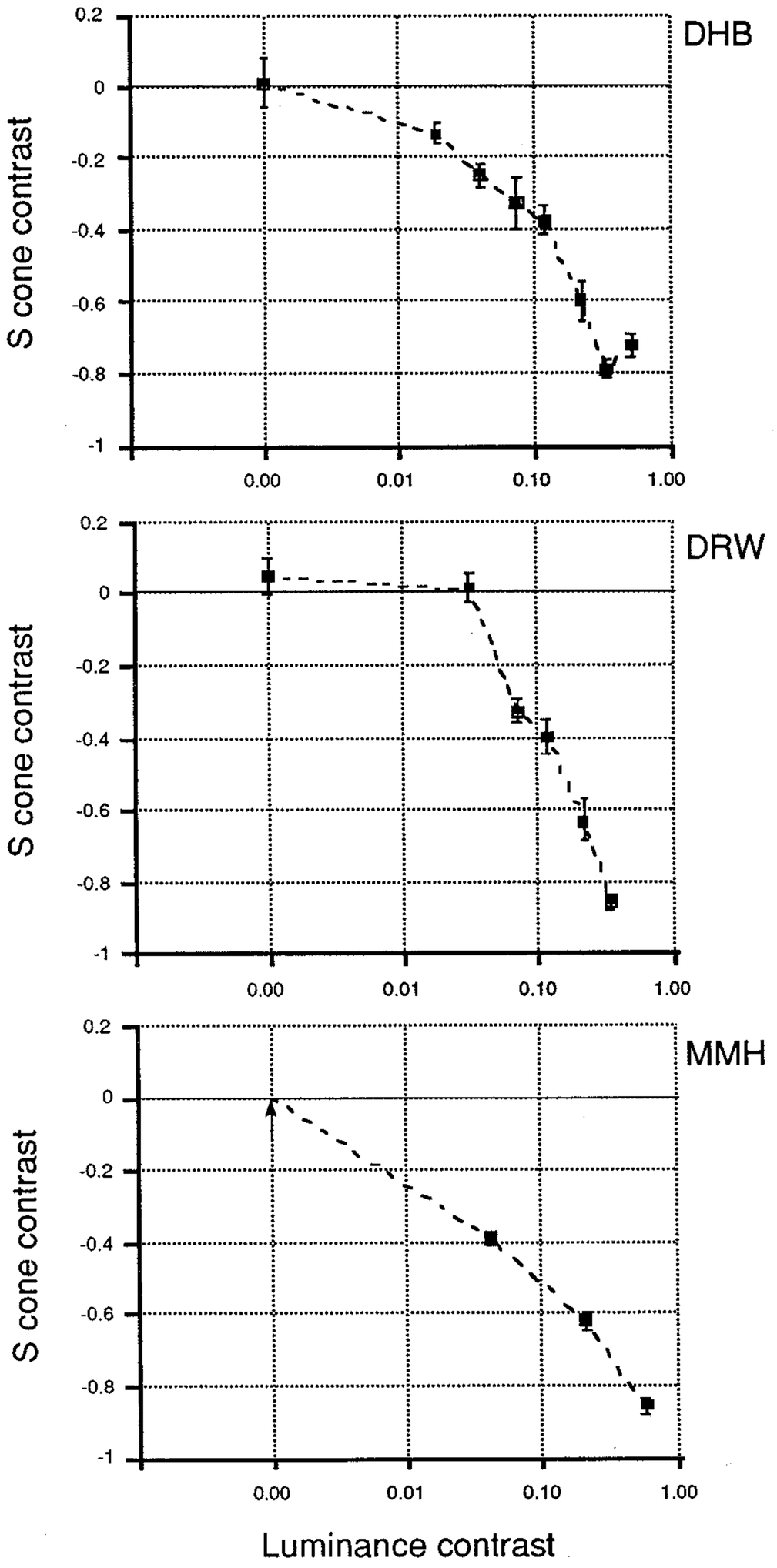

FIGURE 4. Experiment 1 results. Each panel shows results for one observer. The horizontal axis shows the luminance component contrast on a log scale. The vertical axis shows the S cone contrast of the match on a linear scale. See the text for details. (a) Observer DHB. Background luminance, 1310 cd/m^2 (9259.8 td); short-wavelength field luminance, 0.24 cd/m^2 (1.7 td). Comparison disk in temporal visual field. (b) Observer DRW. Background luminance, 1410 cd/m^2 (9966.7 td); short-wavelength field luminance, 0.24 cd/m^2 (1.7 td). Comparison disk in nasal visual field. (c) Observer MMH. Background luminance, 1210 cd/m^2 (8553.0 td); short-wavelength field luminance, 0.17 cd/m^2 (1.2 td). Comparison disk in temporal visual field.

field. A contrast of zero indicates that the matching intensity equaled that of the intensity of the surrounding short-wavelength field. That is, a contrast of zero represents complete filling-in. This level is indicated by the solid horizontal line in each panel. A positive contrast indicates that the matching intensity was an S cone increment, while a negative contrast indicates that the matching intensity was an S cone decrement. A contrast of -1.0 indicates no filling-in whatsoever. The data points in each panel are connected by dashed lines. The error bars show ± 1 SE of the mean match.

Only observers DHB and DRW set matches for the condition where the luminance component contrast was zero. The matches of these two observers confirmed their subjective reports of complete filling-in. For this reason, we did not ask observer MMH to set matches for this condition. Observer MMH also reported good subjective filling-in, and we indicate this with the solid arrow on the graph.

As the luminance component contrast is increased, the pattern of results for all three observers is the same: the amount of filling-in is reduced. These results allow us to reject the separate S cone reconstruction hypothesis.

Control experiments

We considered several alternative explanations for our results, which we rule out as described below.

Eye movements. Systematic failure to maintain fixation could reduce the amount of short-wavelength light required for a comparison disk match. If this were the complete explanation for our results, it is difficult to account for the measured dependence of matching contrast on the luminance component contrast. Furthermore, we found for observer DHB that the luminance component reduced filling-in even when the foveal disk had the same short-wavelength intensity as the surrounding short-wavelength field. In this case, eye movements would allow S cones around the tritanopic area detect the presence of violet there. Yet the blocking of filling-in persisted.

Luminance component contribution to S cone contrast. S cone contrast provided directly by the luminance component at the comparison disk could distort our results, since it would reduce the amount of short-wavelength light required for a match. Calculations suggested that this effect would be very small, which we confirmed for one observer under conditions that produced even better isolation of the luminance component. Observer DHB set matches using a red background (metameric to 615 nm, $x = 0.68$, $y = 0.32$, luminance 451 cd/m^2, 3187.9 td) and luminance component. This luminance component and background provided approx. 2 log units less S cone stimulation than the short-wavelength field. None the less we found that the red luminance component produced similar blocking of tritanopic filling-in.

Effect of macular pigment. We have considered the possibility that spatial variation in the macular pigment across the retina could cause an asymmetry in the amount of short-wavelength light incident at the retina between the foveal and comparison disks. Similarly, there could be spatial non-uniformity in the stimulus itself. Such asymmetries present little problem for our conclusions, which depend on the changes in matches with the addition of the luminance component. Any stimulus asymmetries should have the same effect at all levels of the added luminance component.

EXPERIMENT 2—GRATINGS

Overview

Experiment 1 tested the separate S cone reconstruction hypothesis for the tritanopic area. The fact that L and M cone information did influence S cone reconstruction in Expt 1 suggests that it might also influence the S cone reconstruction of fine gratings. In particular, we were intrigued by the hypothesis that the addition of L and M cone information might allow the veridical perception of S cone gratings that would otherwise be seen as low-frequency aliases. Experiment 2 was designed to examine this hypothesis.

To illustrate the logic of the experiment, Fig. 5 illustrates two pairs of S cone aliases. The two stimuli at the top of the figure are aliases of one another with respect to a model foveal cone mosaic.* Each stimulus consists of a short-wavelength spatial modulation presented against a long-wavelength background. The image on the upper left shows a regular sinusoidal grating. The image on the upper right was constructed from the grating stimulus. To generate the image on the upper right, we computed the S cone responses to a grating stimulus using the model mosaic. We then constructed the stimulus shown on the upper left by applying a bilinear interpolation algorithm (Becker & Chambers, 1984) to the computed cone responses. Thus the two upper stimuli differ only in the gaps between the S cones.

Williams *et al.* (Williams & Collier, 1983; Williams *et al.*, 1983) showed that when observers are presented with gratings such as the one on the upper left of the figure, they report a percept that resembles the stimulus on the upper right. In the absence of L and M cone information, the visual system's reconstruction processes apparently choose a low spatial-frequency alias rather than the veridical high spatial-frequency grating. In Williams *et al.*s' experiment, there was no L and M cone information available about the spatial structure of the stimulus, so that there was no opportunity for the visual system to use L and M cone information to influence its estimate of the S cone stimulus component.

The images on the bottom half of Fig. 5 show a second pair of aliases. This pair was constructed from the stimuli in the top row by superimposing a grating seen only by L and M cones. Since the same grating was superimposed on both left and right, the bottom pair are aliases of one another. At spatial frequencies where S cone aliasing can be observed, the L and M cones are able to veridically resolve the grating. If S cone reconstruction occurs independently of L and M cone signals, then when observers are presented with the grating stimulus shown on the lower left, their percept should resemble the image shown on the lower right. On the other hand, if L and M cone signals play a role in the S cone reconstruction process, observers might experience the veridical grating percept. Indeed, the grating stimulus shown in the figure is a good candidate for revealing any interactions between L and M cone signals and S cone reconstruction, as the L and M cone information perfectly predicts the S cone stimulus component. We reasoned that if there were interactions like those revealed by Expt 1, addition of the L and M cone grating would capture the violet and yellow splotches, leading to veridical grating percept at spatial frequencies above the S cone resolution limit.

In Expt 2, then, our strategy was to arrange conditions where the S cones alone could not correctly resolve a grating and then to add a grating seen by the L and M cones. As in Expt 1, we constructed our stimulus from three components: a background, a short-wavelength component, and a luminance component. The background allowed us to isolate the S cones with short-wavelength light. The use of separate short-wavelength and luminance components allowed us to manipulate the S cone and L and M cone signals independently.

We began by presenting observers with a fine short-wavelength grating against a long-wavelength background, like the stimulus shown in the upper left of Fig. 5. The grating and background both subtended 6 deg of visual angle. As expected, this stimulus was perceived as low-frequency splotches, like the stimulus shown in the upper right of the figure. We then superimposed the luminance component: a long-wavelength grating of the same spatial frequency, orientation, spatial phase, and spatial extent as the short-wavelength grating. This stimulus resembled the lower left panel of the figure. We wanted to know whether the presence of the luminance component modified the splotchy percept towards that of a grating. To measure this, we used a forced-choice orientation discrimination technique. The observer's task was to determine whether the short-wavelength grating was oriented horizontally or vertically. In the absence of L and M cone information, previous studies have shown that this orientation discrimination cannot be performed using the appearance of the splotchy S cone percept (Williams & Collier, 1983; Williams *et al.*, 1983). This is because the aliases of both horizontal and vertical S cone gratings have a similar spatial structure. We reasoned that if the luminance component affected the perceived spatial structure, it would produce an anisotropy in the appearance of horizontal and vertical short-wavelength gratings. We used a forced-choice technique with feedback to maximize our sensitivity to small differences in perceived structure.

Apparatus and stimulus details

Bright high-contrast short-wavelength gratings are required to demonstrate S cone aliasing. We used dual polarization interferometers to produce the short-wavelength and luminance components of the stimulus. The

*The cone locations in the model mosaic were determined by digitizing a photograph of a whole mount of the central 1 deg of a primate retina. The whole mount was provided by Hugh Perry. The assignment of cone types to locations was done as follows. We assigned approx. 9% (407/4352) of the cones to be S cones. The S cones were chosen so that their spatial distribution was about as regular as peripheral mosaic taken as a whole. The remainder of the cones were assigned in a ratio of 2:1 to be L or M cones. We did not include a tritanopic area in the model mosaic.

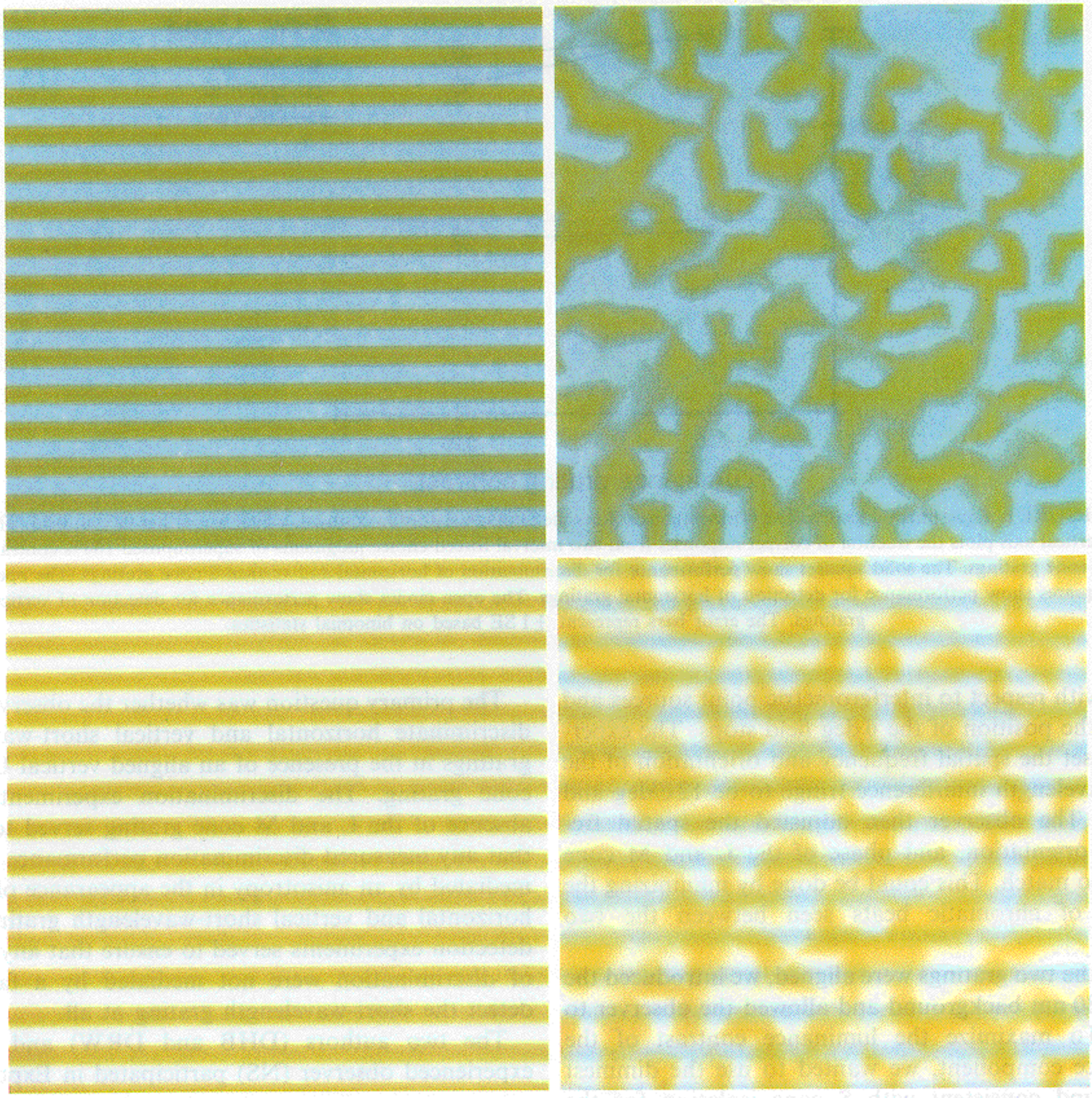

FIGURE 5. S cone alias pairs. See description in the text. Top left, short-wavelength grating. Top right, a low spatial-frequency alias of the grating shown on the top left. Bottom left, a grating that modulates all three cone classes together. Bottom right, an alias of the grating shown on the lower left. These images illustrate the spatial structure of the S cone aliases. Their color appearance does not match that of the actual experimental stimuli.

design of these of interferometers will be described in detail elsewhere (Sekiguchi, Williams & Brainard, 1992). They are in most respects similar to the interferometer described by Williams (1985), but contain important modifications which improve the stability of the interference fringes. The two beams of each interferometer were independently pulsed at 500 Hz. The temporal overlap between pairs of pulses, one from each beam, could be varied to determine the contrast of the interference fringe. This technique allowed contrast to be varied without changing the space-averaged luminance in the field or otherwise introducing artifacts into the stimulus.

The short-wavelength component was produced using 441.6 nm light from 10 mW He–Cd laser. The spatial frequency, orientation, and spatial phase of this interference fringe was under computer control. The luminance component was produced using the 632.8 nm light from a 5 mW He–Ne laser. The spatial phase of this interference fringe was under computer control. The spatial frequency and orientation could be adjusted manually with high precision. The background component was produced by a Quartz lamp arranged in Maxwellian view through a 3 mm artificial pupil conjugate with the natural pupil, rendered monochromatic at 580 nm by a ISA instruments model H10/VIS1200 monochrometer.

Calibration. The stimuli were calibrated with an United Detector Technology model 61 Radiometer, which measured the radiant flux at the pupil. The retinal illuminances of the background, luminance component, and short-wavelength components were 3280, 989, and 1.3 td respectively. The luminance contrast of the luminance component was 0.23 when the 632.8 nm interference fringe was set to 100% contrast.

Procedure

To minimize head movement, the observer's head was held fixed using a dental impression. At the beginning of each session, the observer used an x–y–z stage to align

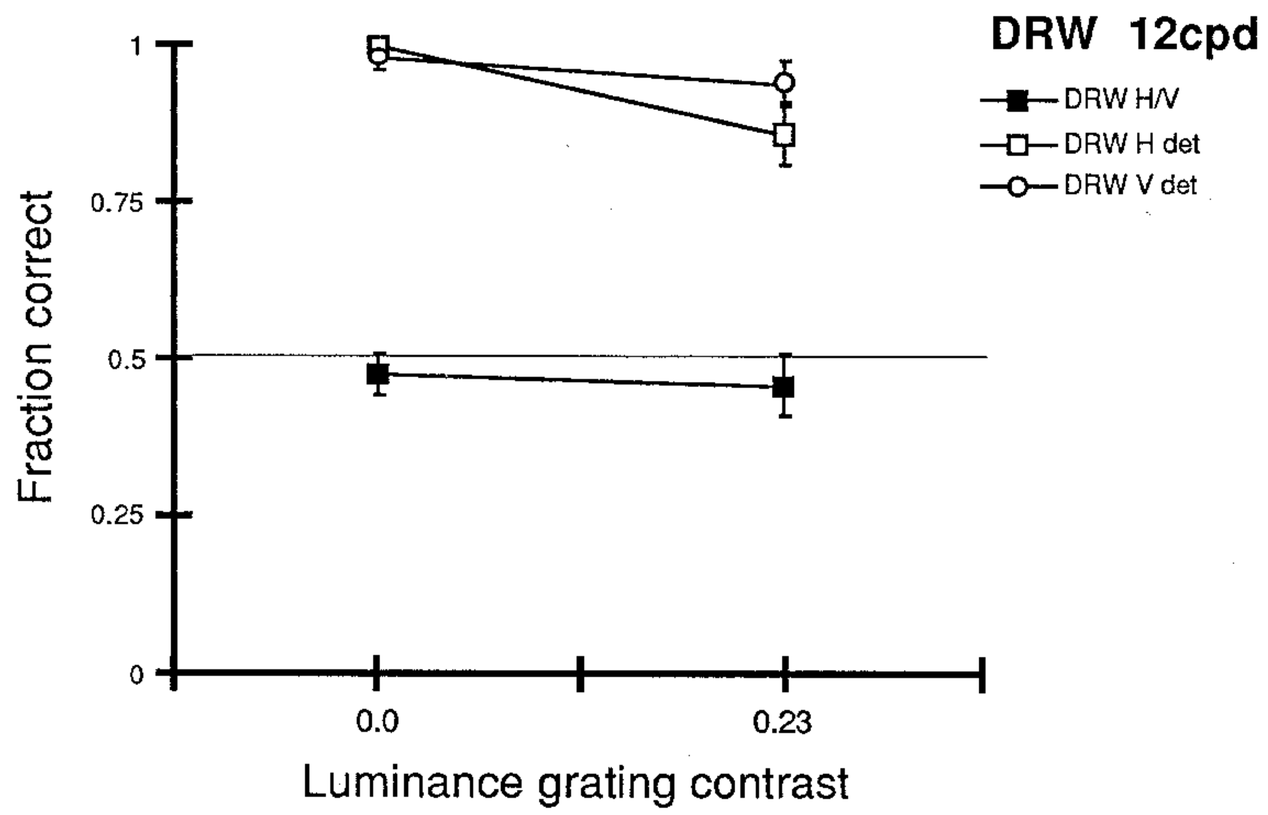

FIGURE 6. Experiment 2 results. The horizontal axis plots the luminance grating contrast, which was either 0.00 to 0.23. The vertical axis plots the fraction of correct responses from two interval forced-choice judgments of superimposed 100% contrast S cone gratings. The solid squares show performance for discrimination of horizontal and vertical S cone gratings. The open squares show performance for detection of horizontal gratings. The open circles show performance for detection of vertical gratings. The error bars represent ±1 SE based on binomial statistics.

his eye with respect to interferometric point sources and aligned the position of the 6 deg field stops. The experimenter set the spatial frequency and orientation of the short-wavelength interference fringe to be 12 c/deg and vertical. The observer then adjusted the spatial frequency, orientation, and phase of the L and M cone grating to match. This could be done by minimizing the number of chromatic beats seen between the two gratings.

After the two gratings were aligned, we introduced the bright 580 nm background and allowed the observer to adapt. To maximize the luminance contrast of the luminance component, we wanted to use the dimmest background consistent with S cone isolation for the short-wavelength grating. To achieve this, we set the contrast of the short-wavelength grating to 100% and the contrast of the L and M cone grating to zero, then allowed the observer to find the minimum background intensity for which he was unable to resolve the orientation of the short-wavelength grating. At this background intensity, a short-wavelength grating in either orientation was detectable as violet and yellow splotches.

After the alignment was complete and the background intensity was set, we conducted a series of forced-choice measurements. First we set the L and M cone grating contrast to 100% and measured how well the observer could detect and discriminate 100% contrast horizontal and vertical short-wavelength gratings. The detection and discrimination were blocked in separate runs. The horizontal and vertical detection trials were intermixed in the same run. We then repeated the same measurements with the L and M cone grating contrast set to zero. The mean luminance of the L and M cone grating was unchanged in this condition. Feedback was given after each forced-choice trial. The stimulus duration was 500 msec for all conditions. The interstimulus interval was determined by the time the observer took to respond to the previous trial.

The primary question was whether the observer could discriminate horizontal and vertical short-wavelength gratings in the presence of an aligned vertical L and M cone grating. The discrimination experiment in the absence of the L and M cone grating served to ensure that any measured discrimination performance was not mediated by an anisotropy in the appearance of aliased horizontal and vertical short-wavelength gratings. The detection experiments served to ensure that any failures of discrimination were not mediated by a failure to detect the short-wavelength grating at all.

The two authors (DHB and DRW) and a third experienced observer (NS) participated in Expt 2.

Results

Figure 6 shows the results of the forced-choice measurements. Observer DRW was not able to discriminate between horizontal and vertical short-wavelength gratings, both in the presence of a L and M cone grating and in the absence of a L and M cone grating. Discrimination performance was at the 50% chance level for both conditions. This indicates a failure of the luminance component to modify the reconstruction of the S cone component. The discrimination failure was not due to a failure to detect the short-wavelength gratings: detection performance for all conditions was well-above threshold.

We were not able to obtain meaningful forced-choice data for the two other observers (DHB and NS). In the absence of a L and M cone grating, both of these observers showed considerable asymmetry in their ability to detect horizontal and vertical short-wavelength gratings. The detection asymmetry prevented us from applying the forced-choice discrimination paradigm for these observers. We do not know the exact cause of the detection asymmetry. Whatever its origin, the asymmetry varies from individual to individual.

We did obtain subjective reports from all three observers about the appearance of the vertical

short-wavelength gratings when they were presented with an aligned L and M cone grating. For all three observers, the presence of the violet grating was differentiated from a uniform violet field of the same mean luminance by the appearance of yellow and violet splotches seen superimposed on the L and M cone gratings. The percept was quite clear and resembled the stimulus shown on the lower right of Fig. 5. Together with the forced-choice results for observer DRW, these subjective reports lead us to conclude that the L and M cone grating does not influence the reconstruction of the S cone signals for these fine grating stimuli.

The appearance of violet gratings

The result of Expt 2 predicts that S cone aliasing should be visible for gratings that modulate all three classes of cones, such as a monochromatic violet grating seen in the dark. Using the interferometric apparatus, we presented four observers (DHB, DRW, NS and a visitor to our laboratory KU) with monochromatic (441.6 nm) 100% contrast 12 c/deg gratings, seen in isolation. All observers reported the appearance of subtle yellow–green splotches superimposed over a resolved grating. Some of the observers also reported that areas of the visual field appeared a deeper violet than others. We also presented three observers (DHB, DRW, and NS) with an 8.6 c/deg 100% contrast monochromatic 440 nm square-wave grating in Maxwellian view. The grating was formed by placing a 100 line-per-in. Ronchi ruling conjugate with the retina in the incoherent channel of the apparatus described for Expt 2. All three observers reported similar splotches for these incoherent gratings.

We want to emphasize that the splotches seen with monochromatic gratings are quite subtle. For the incoherent grating, alignment of the pupil and sharp focus were critical for the observation. For both types of gratings, the splotches were more easily observed when the grating was briefly exchanged with a uniform field of the same wavelength and mean luminance than when it was presented steadily. The visibility of chromatic splotches for high contrast monochromatic gratings serves to control against the possibility that our failure to reveal an interaction in Expt 2 was due to insufficient luminance grating contrast or to imprecise alignment of the two grating components.

The appearance of white light gratings

Chromatic aberration prevents white light gratings from being in sharp focus for all three cone classes simultaneously. Williams *et al.* (1991) demonstrated S cone aliasing using white light gratings by manipulating the accommodative state of the eye to bring the grating into focus for the S cones. They used 20 c/deg gratings and found that when S cone aliasing was visible the luminance grating was near contrast threshold, precluding the possibility of luminance locking. We have experimented with this phenomenon and found that it is possible to choose a grating spatial frequency and accommodative state such that both S cone aliasing and the veridical L and M cone grating are simultaneously visible. For most observers, this can be demonstrated by viewing a white light square-wave transparency of approx. 8–10 c/deg in front of a small accommodative target. Thus a number of quite different experimental conditions all lead to the conclusion that S cone aliasing of fine gratings is not affected by L and M cone information.

DISCUSSION

The corona effect

In Expt 1, we found that luminance disks have a substantial blocking effect on filling-in. In contrast, Williams *et al.* (1981a) report S cone filling-in across a high contrast luminance disk. Their stimulus configuration was quite different from ours. Rather than surrounding the tritanopic area with a uniform short-wavelength field, they used a defocused short-wavelength skirt, which mimicked the pattern of light that would be scattered from a small short-wavelength disk lying inside the tritanopic area. They found that surrounding a small, 20 min in diameter, 519 nm disk with such a skirt had a dramatic effect on its color appearance, changing it from green to blue. Our results (see Fig. 4) show some residual filling-in, so that one way to reconcile the two reports is to assume that partial filling-in can have a strong effect on the color appearance of a 519 nm disk. A second possibility is that surrounding the tritanopic area with a short-wavelength skirt provides stronger filling-in than does surrounding it with a uniform short-wavelength field. Support for this explanation is provided by the fact that the corona effect can also be observed in peripheral retina (Williams, personal communication). Apparently, the filling-in provided by a corona is powerful enough to override the signals provided by the sparse S cone mosaic.*

Border locking

From his study of the appearance of isoluminant red–green stimuli, Gregory (1977) advanced the idea that luminance boundaries constrain the spread of chromatic percepts. Following Gregory, we use the term *border locking* to denote this general idea. In their study of the *gap effect*, Boynton *et al.* (1977) (see also Nick & Larimer, 1983; Eskew & Boynton, 1987; Eskew, 1989) used a discrimination paradigm to argue that border locking occurs between luminance boundaries and S cone signals. The results of Expt 1 are consistent with border locking. We can regard the effect of the

*Here we are adopting Walls' (1954) view that reconstruction processes revealed at retinal blind areas are likely to reflect the action of reconstruction processes that act (albeit more subtly) over the entire visual field. This view is supported by work showing that, under appropriate experimental conditions, filling-in processes can be revealed at retinal regions containing functional photoreceptors. Most of these experiments reveal the filling-in process by stabilizing images on the retina (e.g. Krauskopf, 1963; Yarbus, 1967; Ditchburn, 1973; Piantanida & Larimer, 1989), although more recently other techniques have been developed (Paradiso & Nakayama, 1991; Ramachandran & Gregory, 1991).

luminance disk as segregating the central tritanopic area from the surrounding short-wavelength field, causing the system to estimate what is there separately from the surround. The border locking found in Expt 1 does not extend to the conditions of Expt 2. A border locking view would predict that the perceptual edges provided by the luminance grating should have constrained the reconstructed S cone signals.

One important difference between the stimuli used in Expts 1 and 2 is the spatial scale at which the stimuli vary. Although the tritanopic area is small on an absolute scale, its width corresponds to one bar in a 1.5 c/deg square-wave grating, much coarser than the spatial frequencies at which S cone aliasing occurs for grating stimuli. As we noted in the Introduction, it is sensible for the visual system to use L and M cone information during S cone reconstruction under circumstances where the L and M stimulus components predict the S cone stimulus component. In natural viewing, chromatic aberration makes it unlikely that fine gratings with high retinal contrast for all cone types originate from the same object. Thus there may be few situations in natural viewing where the visual system gains by using L and M cone information to reconstruct very fine structure in the S cone component. Indeed, we believe that it is chromatic aberration that protects us from regularly observing S cone aliasing outside of the laboratory (Yellott, Wandell & Cornsweet, 1984).

What constitutes a border?

The results of Expt 1 allow us to conclude that a complete theory of S cone reconstruction must include a description of the role of L and M cone information. The results of Expt 2 indicate that the nature of the interaction depends on the spatial structure of the stimuli. Using the matching paradigm developed in Expt 1 it is possible to explore this dependence at the tritanopic area. To do this, we can vary the structure of the luminance component and measure how such variation affects the comparison disk matches.

To date, we have made only a few preliminary observations. For observer DHB, we found that luminance decrements had an effect on S cone filling-in similar to that found for luminance increments. As the contrast of the luminance decrement increased, we measured progressively less filling-in. That both increments and decrements reduce filling-in supports the notion that it is the image segregation provided by the luminance component that mediates the interaction. For observers DHB and DRW, we found that for thin luminance rings (18 min of visual angle o.d., 13 min of visual angle i.d.) had a much smaller influence on S cone filling-in than luminance disks with the same outside diameter. This result suggests that the luminance boundary common to both the disk and the ring is not only source of interaction. For observer MMH, on the other hand, the luminance rings were as effective as the luminance disks at blocking filling-in. Both Paradiso and Nakayama (1991) and Ramachandran and Gregory (1991) studied the effects of ring borders on filling-in, but each with quite different stimuli and viewing conditions. Gregory and Ramachandran found that a ring was not as effective as a disk in blocking filling-in. Although they did not make direct comparisons with disks, Paradiso and Nakayama found that a ring blocked filling-in almost entirely.

Gregory (1977) suggested that border information can only be provided by the luminance pathway. Cavanagh (1987), on the other hand, adopted the view that it is only the perceptual salience of a border, rather than its physical origin, that determines its effectiveness. This is consistent with the results of Eskew (1989), who demonstrated the gap effect using an isoluminant red–green boundary. Our experiments used only luminance boundaries and are silent on this issue.

Algorithmic models of the reconstruction process

Recall that we have defined reconstruction as the process or rule by which the visual system chooses one privileged stimulus from each set of aliases. One interesting approach to modeling this process is to use algorithms borrowed from the engineering literature, as suggested by Barlow (1979). These algorithms were originally developed for reconstructing signals from sample values (e.g. Bracewell, 1978; Pratt, 1978; Menke, 1989). To predict appearance, the models compute the responses of the cone mosaic to a stimulus and then generate a perceptual prediction by applying a reconstruction algorithm to the receptor responses. This approach has been used successfully to model the appearance of high spatial-frequency intensity gratings (Yellott, 1982, 1983, 1990; Coletta & Williams, 1987; Williams & Coletta, 1987; Williams, 1988; Ahumada & Yellott, 1989; Coletta *et al.*, 1990).*

A complete account of reconstruction must specify how information from the three classes of cones is combined. In collaboration with Sekiguchi, Haake and Packer, we have previously described a model of the reconstruction of grating stimuli that is based on the assumption that the reconstruction of signals from each class of cone occurs separately (Williams *et al.*, 1991). The results of Expt 2 indicate that this assumption is justified for the S cone submosaic. We have no direct evidence about whether the signals from the L and M cone submosaics are also reconstructed separately.†

*Barlow (1979) also suggested that the reconstruction process might be implemented early in the visual pathway and that a representation of the reconstructed stimulus might exist in primary visual cortex. Although this is an interesting idea, we do not feel that it is a necessary consequence of using signal processing algorithms to model the relation between cone responses and appearance.

†In principle, we could use the logic of Expt 2 to check for interactions between L and M cones. The difficulty is that it has not been possible to demonstrate submosaic aliasing for either L or M cone isolated stimuli. A number of studies (Green, 1968; Carvonious & Estevez, 1975; Packer, Williams, Sekiguchi, Coletta & Galvin, 1989; Williams, 1990) have shown that grating resolution is the same for L or M cone isolated stimuli as it is for the mosaic as a whole. Packer and colleagues (Packer *et al.*, 1989; Williams, 1990) examined the appearance of high-frequency interference fringes under conditions that isolated the L or M cones. They found no difference between the spatial structure of aliases for cone isolated fringes and for fringes that stimulated both L and M cones.

Our separate submosaic reconstruction model predicts that striking red–green splotches should be visible when observers view 20 c/deg intensity gratings. Although such splotches can indeed be seen (Williams *et al.*, 1991), their very low apparent contrast is not consistent with the model's prediction. One way to improve the model may be to allow interactions between the L and M cones (see Freeman, 1987; Ahumada, 1987; Brainard, Wandell & Poirson, 1989).

The signal reconstruction algorithms have the attractive feature that they incorporate an explicit assumption about which stimuli from each set of aliases are most likely to occur in the natural environment. When the assumption is valid, the algorithms provide a normative prescription for accurate reconstruction. A typical assumption is that the retinal image is band-limited in spatial frequency, so that the appropriate reconstruction algorithm is low-pass filtering. This assumption is justified for fine grating stimuli in part because there seems to be little high frequency variation in natural images (Field, 1987) and in part because of the low-pass filtering performed by the optics of the eye (Snyder & Miller, 1977; Campbell & Gubisch, 1966).

In principle, signal reconstructon algorithms can also be used to model filling-in at extended retinal blind areas. The difficulty is to find a suitable assumption about which members from each set of aliases are most likely to occur. The band-limit assumption alone will not provide a sufficient constraint for the more extended blind areas. A recent trend in the engineering literature is to use detected edges to provide additional information about the sampled signal (e.g. Freeman, 1987; Alter-Gartenberg, Huck & Narayanswamy, 1990). This work offers interesting possibilities for formalizing border locking notions. The results of Expt 1 show that to succeed as models of tritanopic area filling-in, such algorithms cannot be applied separately to the responses of each cone submosaic. Interactions between cone classes must be included.

REFERENCES

Ahumada, A. Jr (1987). Aliasing predictions from a spin-glass model for assigning cones to color sensitivity classes. *Investigative Ophthalmology and Visual Science (Suppl.), 28,* 137.

Ahumada, A. J. Jr & Yellott, J. I. Jr (1989). Reconstructing irregularly sampled images by neural networks. *Proceedings of the SPIE Symposium on Human Vision, Visual Processing, and Digital Display, 1077,* 228–235.

Alter-Gartenberg, R., Huck, F. O. & Narayanswamy, R. (1990). Image recovery from edge primitives. *Journal of the Optical Society of America A, 7,* 898–911.

Barlow, H. B. (1979). Reconstructing the visual image in space and time. *Nature, 279,* 189–190.

Becker, R. A. & Chambers, J. M. (1984). *S: An interactive environment for data analysis and graphics.* Belmont, Calif.: Wadsworth Advanced Book Program.

Boynton, R. M., Hayhoe, M. M. & MacLeod, D. I. A. (1977). The gap effect: Chromatic and achromatic visual discrimination as affected by field separation. *Optica Acta, 24,* 159–177.

Bracewell, R. (1978). *The Fourier transform and its applications.* New York: McGraw-Hill.

Brainard, D. H., Wandell, B. A. & Poirson, A. B. (1989). Discrete analysis of spatial and spectral aliasing. *Investigative Ophthalmology and Visual Science (Suppl.), 30,* 53.

Campbell, F. W. & Gubisch, R. W. (1966). Optical quality of the human eye. *Journal of Physiology, 186,* 558–578.

Cavanagh, P. (1987). Reconstructing the third dimension: Interactions between color, texture, motion, binocular disparity, and shape. *Computer Vision, Graphics, and Image Processing, 37,* 171–195.

Cavonius, C. R. & Estevez, O. (1975). Contrast sensitivity of individual colour mechanisms of human vision. *Journal of Physiology, 248,* 649–662.

Cole, G. R., Stromeyer, C. F. III & Kronauer, R. E. (1990). Visual interactions with luminance and chromatic stimuli. *Journal of the Optical Society of America A, 7,* 128–140.

Coletta, N. J. & Williams, D. R (1987). Psychophysical estimate of extrafoveal cone spacing. *Journal of the Optical Society of America, 4,* 1503–1513.

Coletta, N. J., Williams, D. R. & Tiana, C. L. M. (1990). Consequences of spatial sampling for human motion perception. *Vision Research, 30,* 1631–1648.

Curcio, C. A., Allen, K. A., Sloan, K. R., Lerea, C. L., Jurley, J. B., Klock, I. B. & Millam, A. H. (1991). Distribution and morphology of human cone photoreceptors stained with anti-blue opsin. *Journal of Comparative Neurology, 312,* 610–624.

deMonasterio, F. M., McCrane, E. P., Newlander, J. K. & Schein, S. J. (1985). Density profile of blue-sensitive cones along the horizontal meridian of Macaque retina. *Investigative Ophthalmology and Visual Science, 26,* 289–302.

Ditchburn, R. W. (1973). *Eye-movements and visual perception.* Oxford: Clarendon Press.

Eskew, R. T. Jr (1989). The gap effect revisited: Slow changes in chromatic sensitivity as affected by luminance and chromatic borders. *Vision Research, 29,* 717–729.

Eskew, R. T. Jr & Boynton, R. M. (1987). Effects of field area and configuration on chromatic and border discriminations. *Vision Research, 27,* 1835–1844.

Field, D. J. (1987). Relations between the statistics of natural images and the response properties of cortical cells. *Journal of the Optical Society of America A, 4,* 2379–2394.

Freeman, W. (1987). Method and apparatus for reconstructing missing color samples. United States Patent 4663655.

Green, D. G. (1968). The contrast sensitivity of the colour mechanisms of the human eye. *Journal of Physiology, 196,* 415–429.

Gregory, R. L. (1977). Vision with isoluminant colour contrast: 1. A projection technique and observations. *Perception, 6,* 113–119.

Helmholtz, H. (1896). *Physiological optics.* New York: Dover.

Kanizsa, G. (1979). *Organization in vision.* New York: Praeger Publishers.

Kawabata, N. (1983). Global interactions in perceptual completion at the blind spot. *Vision Research, 23,* 275–280.

Kersten, D. (1987). Predictability and redundancy of natural images. *Journal of the Optical Society of America A, 4,* 2395–2400.

Koh, K. & Maloney, L. T. (1988). Visual interpolation and extrapolation of linear and quadratic contours through discrete points. *Investigative Ophthalmology and Visual Science (Suppl.), 29,* 408.

Krauskopf, J. (1963). Effect of retinal image stabilization on the appearance of heterochromatic targets. *Journal of the Optical Society of America, 53,* 741–744.

Marr, D. (1982). *Vision.* San Francisco, Calif.: W. H. Freeman.

Menke, W. (1989). *Geophysical data analysis: Discrete inverse theory.* San Diego, Calif.: Academic Press.

Nakayama, K., Shimojo, S. & Silverman, G. H. (1989). Stereoscopic depth: Its relation to image segmentation, grouping, and the recognition of occluded objects. *Perception, 18,* 55–68.

Nick, J. & Larimer, J. (1983). Yellow-blue cancellation on yellow fields: Its relevance to the two-process theory. In *Color vision* (pp. 375–383). London: Academic Press.

Nyman, G. & Laurinen, P. (1982). Reconstruction of spatial information in the human visual system. *Nature, 297,* 324–325.

Packer, O., Williams, D. R., Sekiguchi, N., Coletta, N. J. & Galvin, S. (1989). Effect of chromatic adaptation on foveal acuity and aliasing. *Investigative Ophthalmology and Visual Science (Suppl.), 30,* 53.

Paradiso, M. A. & Nakayama, K. (1991). Brightness perception and filling-in. *Vision Research, 31,* 1221–1236.

Piantanida, T. & Larimer, J. (1989). The impact of boundaries on color: Stabilized image studies. *Journal of Imaging Technology, 15,* 58–63.

Pratt, W. K. (1978). *Digital image processing.* New York: Wiley.

Ramachandran, V. S. & Gregory, R. L. (1991). Perceptual filling in of artificially induced scotomas in human vision. *Nature, 350,* 699–702.

Sekiguchi, N., Williams, D. R. & Brainard, D. H. (1992). Foveal resolution at isoluminance. In preparation.

Snyder, A. W. & Miller, W. H. (1977). Photoreceptor diameter and spacing for highest resolving power. *Journal of the Optical Society of America, 67,* 696–698.

Walls, G. L. (1954). The filling-in process. *American Journal of Optometry, 31,* 329–340.

Williams, D. R. (1985). Aliasing in human foveal vision. *Vision Research, 25,* 195–295.

Williams, D. R. (1988). Topography of the foveal cone mosaic in the living human eye. *Vision Research, 28,* 433–454.

Williams, D. R. (1990). The invisible cone mosaic. In *Advances in photoreception.* Washington, D.C.: National Academy Press.

Williams, D. R. & Coletta, N. J. (1987). Cone spacing an the visual resolution limit. *Journal of the Optical Society of America, 4,* 1514–1523.

Williams, D. R. & Collier, R. J. (1983). Consequences of spatial sampling by a human photoreceptor mosaic. *Science, 221,* 385–387.

Williams, D. R., Collier, R. J. & Thompson, B. J. (1983). Spatial resolution of the short-wavelength mechanism. In *Colour vision* (pp. 487–503). New York: Academic Press.

Williams, D. R., MacLeod, D. I. A. & Hayhoe, M. (1981a). Foveal tritanopia. *Vision Research, 21,* 1341–1356.

Williams, D. R., MacLeod, D. I. A. & Hayhoe, M. (1981b). Punctate sensitivity of the blue sensitive mechanism. *Vision Research, 21,* 1357–1375.

Williams, D. R., Sekiguchi, N., Haake, W., Brainard, D. H. & Packer, O. (1991). The cost of trichromacy for spatial vision. In *From pigments to perception.* New York: Plenum Press.

Wyszecki, G. & Stiles, W. S. (1982). *Color science.* New York: Wiley.

Yarbus, A. L. (1967). *Eye movements and vision.* New York: Plenum Press.

Yellot, J. I. Jr (1982). Spectral analysis of spatial sampling by photoreceptors: Topological disorder prevents aliasing. *Vision Research, 22,* 1205–1210.

Yellot, J. I. Jr (1983). Spectral consequences of photoreceptor sampling in the rhesus monkey. *Science, 221,* 383–385.

Yellott, J. I. Jr (1990). The photoreceptor mosaic as an image sampling device. In *Advances in photoreception.* Washington, D.C.: National Academy Press.

Yellot, J. I. Jr, Wandell, B. A. & Cornsweet, T. N. (1984). The beginnings of visual perception: The retinal image and its initial encoding. In *Handbook of physiology: The nervous system* (pp. 257–316). New York: Easton.

Acknowledgements—We thank A. Ahumada, J. Foley, K. Koh, N. Sekiguchi, O. Packer, and B. Wandell for useful discussions or comments on earlier visions of this paper. M. Hayhoe and N. Sekiguchi volunteered to observe in some of the experiments. N. Sekiguchi provided technical support for Expt 2. W. Haake assisted with software development. A preliminary report was presented at the Association for Research in Vision and Ophthalmology 1991 Annual Meeting. Support was provided by NIH EY06278, EY04367, EY00269, EY01319, and AFOSR 88-092.